

Journal of Materials Chemistry A

Accepted Manuscript



This is an *Accepted Manuscript*, which has been through the Royal Society of Chemistry peer review process and has been accepted for publication.

Accepted Manuscripts are published online shortly after acceptance, before technical editing, formatting and proof reading. Using this free service, authors can make their results available to the community, in citable form, before we publish the edited article. We will replace this *Accepted Manuscript* with the edited and formatted *Advance Article* as soon as it is available.

You can find more information about *Accepted Manuscripts* in the [Information for Authors](#).

Please note that technical editing may introduce minor changes to the text and/or graphics, which may alter content. The journal's standard [Terms & Conditions](#) and the [Ethical guidelines](#) still apply. In no event shall the Royal Society of Chemistry be held responsible for any errors or omissions in this *Accepted Manuscript* or any consequences arising from the use of any information it contains.

ARTICLE

Green Preparation of Tuneable Carbon-Silica Composite Materials from Wastes

Cite this: DOI: 10.1039/x0xx00000x

Tengyao Jiang,^a Vitaliy L. Budarin,^a Peter S. Shuttleworth,^b Gary Ellis,^b Christopher M.A. Parlett,^c Karen Wilson,^c Duncan J. Macquarrie^a and Andrew J. Hunt^{*a}

Received 00th January 2012,
Accepted 00th January 2012

DOI: 10.1039/x0xx00000x

www.rsc.org/

Bio-oil has successfully been utilized to prepare carbon-silica composites (CSCs) from mesoporous silicas, such as SBA-15, MCM-41, KIT-6 and MMSBA frameworks. These CSCs comprise a thin film of carbon dispersed over the silica matrix and exhibit porosity similar to the parent silica. The surface properties of resulting materials can be simply tuned by the variation of preparation temperatures leading to a continuum of functionalities ranging from polar hydroxyl rich surfaces to carbonaceous aromatic surfaces, as reflected in solid state NMR, XPS and DRIFT analysis. N₂ porosimetry, TEM and SEM images demonstrate that the composites still possess similar ordered mesostructures to the parent silica sample. The modification mechanism is also proposed: silica samples are impregnated with bio-oils (generated from the pyrolysis of waste paper) until the pores are filled, followed by the carbonization at a series of temperatures. Increasing temperature leads to the formation of a carbonaceous layer over the silica surface. The complex mixture of compounds within the bio-oil (including those molecules containing alcohols, aliphatics, carbonyls and aromatics) gives rise to the functionality of the CSCs.

Introduction

Porous carbonaceous materials have played an important role in many fields of modern science and technology, such as separation processes, electronics, energy storage, biomedical devices and more.^{1, 2} Therefore, a novel family of ordered mesoporous carbon materials designated as CMK series was firstly investigated by Ryoo et al in 1999.^{3, 4} The standard preparation procedure of this material involves the infiltration of mesoporous silica pores with mono- and di-saccharides, followed by their carbonization and silica removal. One of the advantages of this carbonization technique is that the resultant carbon materials could replicate the inverse mesostructural order after removing the silica templates with HF or NaOH solution. Further studies were carried out on the modification of CMK with crosslinked polymers or metals to form chemically enhanced carbon materials.⁵⁻⁷

However, while relevant research focused predominantly on the preparation of porous carbonaceous materials,⁸⁻¹⁰ far less has been published on the investigation of carbon-silica intermediate product. Hence, the carbon-silica composite (CSC) would be the main target in this paper. CSCs are prepared from bio-oil derived via microwave pyrolysis of waste paper, which is subsequently impregnated into the pores of a range of nanostructured silicas, followed by carbonization under a nitrogen atmosphere. This novel route allows the composite to

retain the porosity characteristics of parent silica, but by attaching a thin carbonaceous film on the surface gives great control over the surface polarity. In this case, the silica mesostructure feature could be well controlled and retained via new synthesis route. In contrast to the previous method, mesoporous materials with carbonaceous surfaces can be prepared via a short and cost effective synthesis route. The incorporation of carbon onto silica pore wall not only results in interesting mesoporous carbon-silica composites, but provide a mechanically or chemically enhanced carbonaceous material.¹¹⁻¹⁵ The presence of the rigid silica framework in the composites could also greatly reduce structural shrinkage during high temperature pyrolysis.¹⁶ As such, this highly conductive and porous composite may offer great opportunities for a variety of potential applications in electronics, chemical sensors and heterogeneous catalysis.^{14, 15}

Many carbon materials have been synthesised from biomass, typically through hydrothermal carbonization, or pyrolysis.¹⁷⁻²⁰ The challenges in this field are particularly the control of the porosity of the material and the tuning of graphitic content due to the utilization of biomass as starting materials. Conventional carbon sources used for synthesis of CSC are frequently pure chemicals and polymers such as (poly)furfural alcohol (PFA),^{21, 22} dichloromethane,²³ and sugars (sucrose).¹ However, drawbacks such as toxicity, using products that compete with

food and those that are highly purified may restrict the further development of carbon nanomaterials.²⁴⁻²⁶ Therefore, it is important to identify carbon sources derived from waste that do not require purification, can easily undergo self-polymerization and do not compete with food. Bio-oil is obtained by microwave fast pyrolysis of a range of biomass types, including wood, rice husk, waste paper and so on. Until now, it has been utilized both as an energy source for substitution of conventional fossil fuel and as a feedstock for chemical production with further separation. Bio-oils usually contain many types of oxygenated compounds with various chemical properties, such as aldehydes, ketones, phenols, esters, sugars, furans and multifunctional groups (see Supplementary information - Fig. S1).²⁷⁻³¹ Its polymerization feature is preferably applied in the carbonaceous materials' preparation. Herein, an upgraded application of bio-oil as an environmentally sustainable and economically viable carbon source for fabrication of this composite has been explored.

The prospective vision of this preparation method is illustrated in Fig. 1.

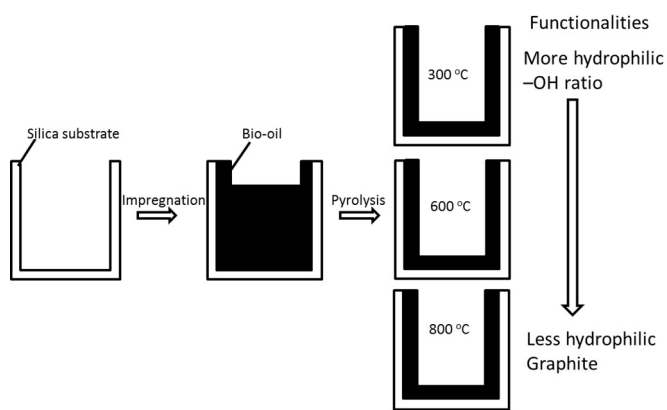


Fig. 1 Proposed mechanism of oil modification on the surface of silica materials

Initially the parent SBA-15 materials are impregnated with bio-oil diluted with specific amount of acetone, followed by evaporation of the solvent and carbonization of the mixture of preparation. The carbon species in the materials vary significantly based on the carbonization temperature, resulting in a continuum functionality ranging from polar hydroxyl groups to aromatic surfaces of CSC. This creates unique advantages compared to traditional synthesis methods. Due to the strong interactions between oxygenated compounds existed in bio-oil and residual silanol groups in silicas, the organic compound not in close contact with silica surface could be more easily removed via increasing temperature, hence a carbonaceous layer is coated around internal side of silica pores. The resultant CSC exhibits not only similar pore structural ordering as parent SBA-15, but also unique advantages including temperature-dependent surface functionality, cost-effective carbon source from waste and is prepared from a simple modification process. In order to

fabricate different types of carbon-silica hybrid materials with specific mesostructure, a variety of porous silica has been utilized as alternative substrates including SBA-15 series in this approach. Several analytical techniques such as X-ray diffraction (XRD), N₂ porosimetry, microscopy, diffuse reflectance infrared fourier transform (DRIFT), solid state NMR, and X-ray photoelectron spectroscopy (XPS) were utilized for characterizing the final product.

Experimental Section

SBA-15 synthesis

The parent SBA-15 was synthesized according to the method published in 1998 by Zhao.³² In a typical synthesis, amphiphilic triblock copolymer, poly(ethylene glycol)-block-poly(propylene glycol)-block-poly(ethylene glycol) (Pluronic P123), was dissolved in HCl solution, followed by the addition with stirring of tetraethylorthosilicate (TEOS) to the homogeneous solution. The gel mixture was stirred overnight and aged at 100 °C for another 24 hours. The solid product was then filtered, washed with deionized water, dried and finally calcined in air flow at the heating rate of 1 °C min⁻¹. The resultant white powder was used as the substrate for the further modification.

KIT-6 synthesis

KIT-6 was produced using the procedure reported by Kim and co-workers.³³ Pluronic P123 (10 g) was dissolved in water (361.6 cm³), Butan-1-ol (12.3 cm³) and hydrochloric acid (35%, 16.7 cm³) with stirring at 35 °C. Tetraethoxysilane (23.6 cm³) was added and left for 20 h with agitation. The resulting gel was aged under sealed conditions for 24 h at 80 °C without agitation. The solid was filtered, washed with water (1000 cm³) and dried at room temperature before calcination at 500 °C for 6 h in air (ramp rate 1 °C min⁻¹).

Macro-mesoporous SBA-15 synthesis

Macro-mesoporous SBA-15 silica (MMSBA) was synthesised via a modified route which incorporated a hard macropore template of polystyrene spheres.

Polystyrene sphere were synthesised using the emulsion polymerisation method of Vandreuil and co-workers.³⁴ Potassium persulfate (0.16 g) was dissolved in distilled water (12 cm³) at 70 °C. In a separate 500 cm³ three-necked round bottomed flask distilled water (377 cm³) was purged under flowing nitrogen (10 cm³ min⁻¹) at 70 °C. Styrene (50 cm³) and divinylbenzene (9.5 cm³) were each washed three times with sodium hydroxide solution (0.1 M, 1:1 vol/vol) followed by three washings with distilled water (1:1 vol/vol) to remove the polymerisation inhibitors. The washed organic phases were added to the purged water followed by the potassium persulfate solution. The mixture was left to stir under nitrogen (10 cm³ min⁻¹) for 15 h, filtered and washed three times with distilled water (100 cm³) and then three times with ethanol (100 cm³).

The silica support was produced using the methodology published by Dhainaut and co-workers.³⁵ Pluronic P123 (10 g) was dissolved in water (75 cm³) and hydrochloric acid (2 M, 290 cm³) with stirring at 35 °C. Polystyrene beads (45 g) were added to the solution and left to stir for 1 h. Tetraethoxysilane (23.5 cm³) was added and left for 20 h with agitation. The resulting gel was aged under sealed conditions for 24 h at 80 °C under static conditions. The solid was filtered, washed with water (1000 cm³) and dried at room temp before calcination at 550 °C for 6 h in air (ramp rate 0.5 °C min⁻¹).

Bio-oil preparation

Bio-oil was prepared through microwave pyrolysis at 1200 psi for 10 minutes. Waste paper was weighed into the microwave vessel and placed in the microwave. The sample was heated from 40 °C to 200 °C under vacuum. Volatile components were collected after condensation.

Carbon-silica composite preparation

Carbon groups were loaded into SBA-15 by wet impregnation process. A solution was prepared by dissolving different amounts of bio-oil into the desired amount of acetone, followed by the addition of various porous supports. After stirring overnight, the solution was then carbonized at a series of different temperatures at a heating rate of 1 °C/min under nitrogen flow to carbonize bio-oil, and finally the carbon-silica composites were obtained. A series of different ratio of bio-oil/silica have been investigated at 500 °C. When the ratio of bio-oil/SBA was 4:1 the porosimetry data showed that this CSC had a significant pore volume (>0.30 cm³ g⁻¹) and pore size of >2.5 nm. As such, this demonstrates that no excess of bio-oil was employed during the process (shown in Supplementary information - Table S1). In the case of when the bio-oil/SBA was 8:1 complete blocking of the pore structure was achieved indicating an excess presence of bio-oil.

Materials Characterization

A Bruker-AXS B8 Advance diffractometer with a Kristalloflex 760 X-ray generator which produces monochromatic K α X-rays from a copper source was employed to obtain XRD patterns. Nitrogen adsorption/desorption analyses were carried out at 77 K using a Micromeritics ASAP 2020 analyzer. Transmission electron microscopy (TEM) images were taken using an FEI Tecnai 12 G2 microscope. Solid-state ¹³C and ²⁹Si NMR (nuclear magnetic resonance) experiments were performed on a Varian VNMRs spectrometer. Spectral referencing was with respect to neat, external tetramethylsilane. ²⁹Si NMR spectra were measured at 79.4 MHz with 30 s recycle delay, and ¹³C NMR spectra were measured at 100.5 MHz with a 1 s recycle delay. XPS measurement were performed on a Kratos Axis HSi spectrometer equipped with a monochromatic Al K α X-ray source and charge neutraliser.

Results and discussion

Textural properties of CSCs

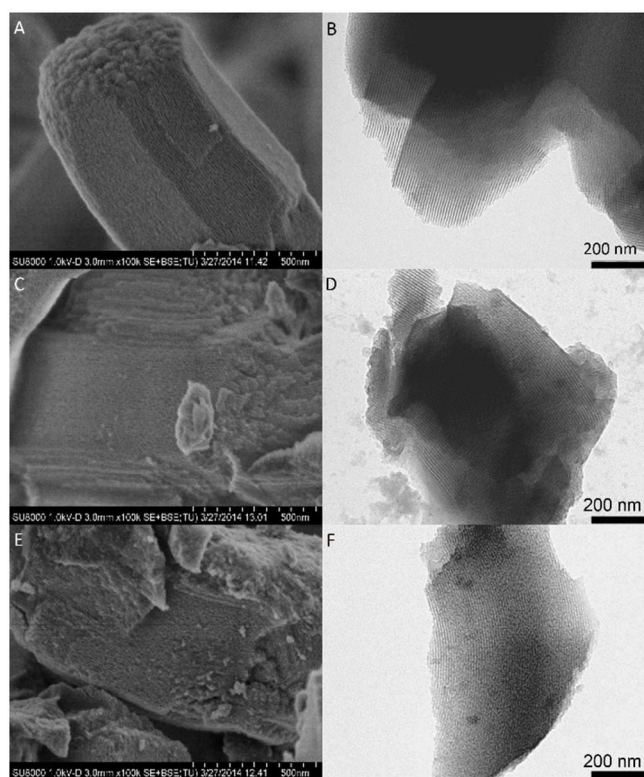


Fig. 2 HRSEM images (left column) and TEM images (right column) of SBA-15 (A, B), CSC-600 (C, D) and CSC-800 (E, F) materials

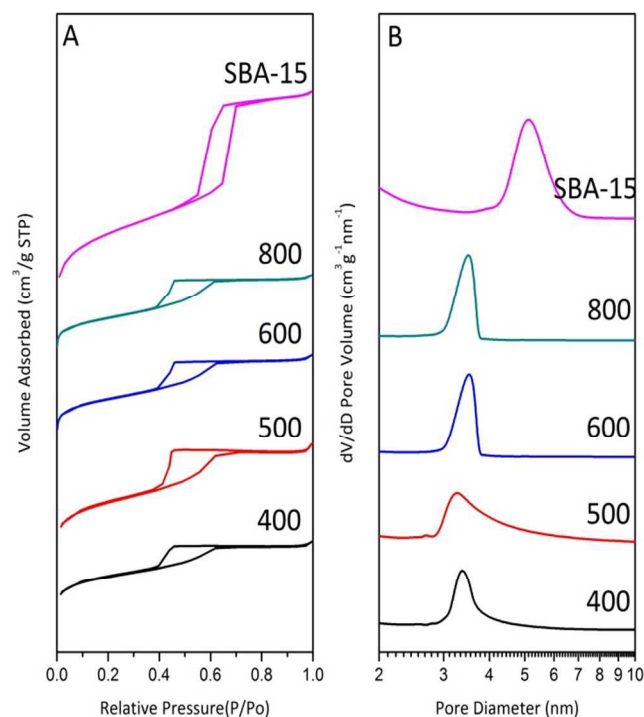


Fig. 3 N₂ adsorption/desorption isotherm plots (A) and pore size distribution (B) of the carbon-silica composites and SBA-15 materials

The proposed mechanism for the formation of materials with increasing temperature is illustrated in Fig. 1. The scanning electron microscopy (SEM) and transmission electron microscopy (TEM) images in Fig. 2 allow observation of the structural ordering of samples and they clearly reveal that the composites exhibits a highly ordered hexagonal mesostructure,

thus retaining the structural order characteristic of the parent silica (magnified TEM images shown in Supplementary information - Fig. S2). SEM images demonstrate that the uniform silica pore channels still exist in the CSCs. The estimated pore diameter measured from the TEM images are approximately 3.75 nm, 3.40 nm and 3.35 nm for parent SBA-

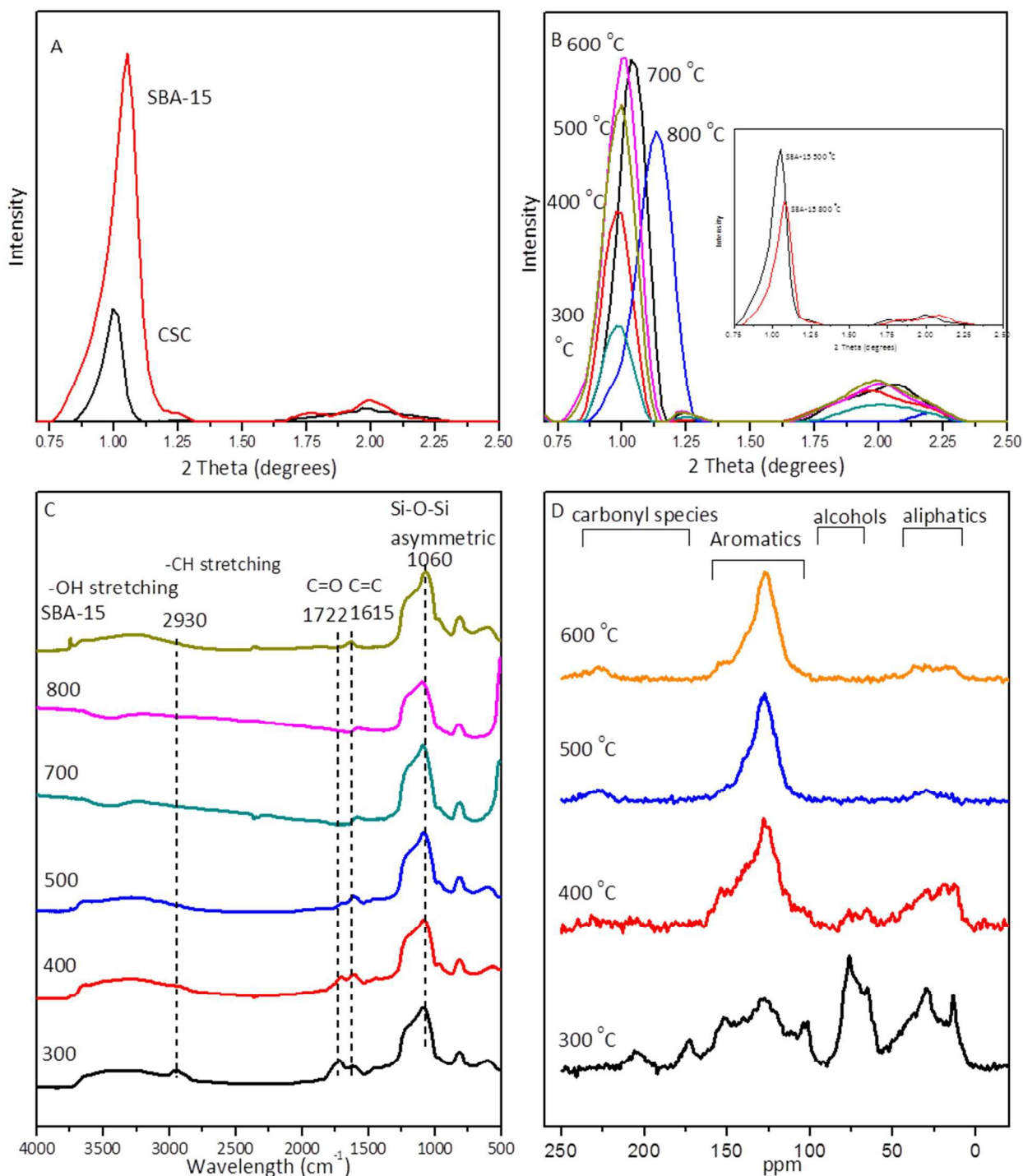


Fig. 4 A) XRD patterns of parent SBA-15 materials and CSC-500. B) XRD patterns of CSC-300, CSC-400, CSC-500, CSC-600, CSC-700 and CSC-800 materials (inset: XRD patterns of SBA-15 materials heated at 500 °C and 800 °C under nitrogen flow). C) DRIFT spectra of the carbon-silica composites and SBA-15 samples. D) ¹³C solid state MAS/NMR spectra of CSC-300, CSC-400, CSC-500 and CSC-600 materials.

15, the carbon-silica composite subjected to pyrolysis at 600 °C (CSC-600) and 800 °C (CSC-800), respectively.³⁶ These results are in good correlation with porosity data from the N₂ adsorption/desorption isotherms (Shown in Supplementary information - Table S2), indicating that carbon-containing species did not affect the mesostructure of the silica substrate dramatically.

Nitrogen adsorption isotherm plots (Fig. 3A) indicate that SBA-15 exhibits a typical type-IV isotherm plot with an H₁-type hysteresis loop, and a steep capillary condensation step in adsorption branch implies a uniform mesopore size.³⁷ However, all the carbon-silica composites carbonized above 400 °C display H₂-type hysteresis loop with a gradual rise in adsorption branch during capillary condensation, revealing a broader pore size distribution and / or non-uniform pore structure.¹⁵ The CSC-300 has an incomplete hysteresis loop (not shown in Fig. 3A) and the BET specific surface area is extremely low at 39 m² g⁻¹ supporting the theory that the silica pores have been fully filled with bio-oils and the carbon source has not been removed at this temperature, and that little shrinkage of the carbonaceous system has occurred. The pore size distributions (Fig. 3B) were calculated using the desorption branch, showing a narrow pore size distribution for all materials. Compared to SBA-15, the composites possess a smaller mesopore size. CSC-300 sample also shows no significant peak in the pore size distribution providing further evidence that the silica pores were filled with polymerised bio-oils as highlighted in Fig. 1.

The XRD patterns (shown in Fig. 4.A) of CSC and its parent SBA-15 provide further evidence that the inorganic structure of the SBA-15 silica remains intact after bio-oil modification process, which could be deduced from microscopy images. The pattern of CSC matches well with that of SBA-15 indexed to a hexagonal lattice,^{38, 39} except the decreased intensity of the peak of CSC due to a ratio change in the contrast between silica/empty space and silica/carbon.⁴⁰

Tunable surface functionalities depending on carbonization temperatures

Fig. 4B demonstrates the comparisons of XRD patterns of CSCs carbonized at 300 °C, 400 °C, 500 °C, 600 °C, 700 °C and 800 °C. The (100) diffraction peak of the materials shifts to larger 2θ degree with the increase of temperature, indicating a smaller interplanar distance d_{100} and a smaller corresponded unit cell.^{37, 38} This is attributed to the shrinkage of silica structure during the carbonization. A control experiment of XRD analysis of pure silica materials heated at 500 °C and 800 °C under nitrogen flow has also been carried out to further prove this phenomenon (Fig. 4B inset). Moreover, the shift of CSCs is more significant than that of silica sample, indicating that not only the shrinkage of silica itself, but also the acids and water from bio-oils could accelerate the crosslink effect of silanol groups.

The intensities of the peaks in XRD pattern increase first as the temperature increases to 700 °C, proving that the temperature rise has a positive effect on the composite structural ordering.⁴⁰ The strong increase of the intensities is

explained by the removal of organic species from the inside of the mesopores and allow to form a more uniform carbonaceous layer. As indicated in Fig. 1, the pores were filled with organic compounds at lower temperature at first. Then some of organic species could decompose with the increase of temperature and a uniform layer containing the chemically stable compounds formed by coating with silica surface. Hence, the XRD result could strongly prove the validity of successful fabrication of carbonaceous silica composite.

The characteristic of continuous functionality depending on different pyrolysis temperature is clearly shown in DRIFT spectra (shown in Fig. 4C). 300 °C sample as the lowest carbonization temperature, contained a variety of functional groups, such as OH groups, C-H groups, C=O groups and C=C groups. As the temperature increases by 800 °C, the functionalities of the material converted to aromatic form. Weakening or disappearance of the peak at 2930 cm⁻¹ assigned to CH stretching indicates that the aliphatic chains decompose completely above 500 °C. The existence of C=O groups from acid, ester, ketone or aldehydes could be confirmed by the peak at around 1720 cm⁻¹. On carbonization from 500 °C this peak disappears, indicating the decomposition of C=O containing species at high temperature. As mentioned, most previous research investigated the carbon-silica fabrication by utilizing soluble resin polymers or sugars as carbon precursor.^{14-16, 36} However, due to the use of pure chemicals and carbonization at certain temperature, the typical product only possesses a carbonaceous layer with a single functionality on the silica surface and the surface property could not become temperature-dependent. In this work, it has been demonstrated that the surface properties of CSCs continually change from polar hydroxyl groups to aromatic surfaces with the increase of pyrolysis temperature. In addition, DRIFT analysis further proved of the existence of silica substrates in CSCs. Three silica characteristic peaks shown at 3500 cm⁻¹, 1060 cm⁻¹ and 800 cm⁻¹ in the spectra of CSCs match well to the parent SBA-15 except for the OH peak.⁴¹ The elimination of OH group in CSC is due to the crosslink effect of silicas under high temperature above 500 °C leading to the OH group loss. It is worthwhile to note that due to the existence of alcohols in CSC-300 sample and CSC-400 sample from ¹³C NMR analysis (detailed below), the peak at 3500 cm⁻¹ should also be assigned to alcohols.

The sample information on the carbon speciation was also indicated from ¹³C MAS/NMR spectra (Fig. 4D) of the carbon silica composites carbonized at 300 °C, 400 °C, 500 °C and 600 °C. CSC-800 (800 °C) sample could not be analysed due to the highly conductivity of the material, thus resulting in the inability to properly tune the probe. This phenomenon exactly implies that high temperature CSCs could be applied in electrochemistry, chemical sensor and nano-electronic applications.^{15, 42} The NMR spectra of 300 °C sample indicated that a wide range of organic functionalities are still present, including ketones at *ca.* 205 ppm, acid/esters at *ca.* 165 ppm, aromatics at *ca.* 150 ppm, alcohols at *ca.* 60 ppm and aliphatics at *ca.* 20 ppm. The data for these functional groups was

consistent with DRIFT analysis above. The 400 °C sample is dominated by increased aromatic character accompanied by aliphatic and alcohol groups. It is evident that the disappearance of characteristic peak at 165 ppm and 205 ppm indicated the decomposition of carbonyl species by 400 °C, and most of alcohols decomposed at the same time evidenced by the decreased intensity of the peak at 76 ppm. In terms of CSC-500 (500 °C) and CSC-600 (600 °C) sample, the aromatic peak (plus spinning sidebands) is the only signal except a weak aliphatic signal around 10-20 ppm, indicating the carbon species were mostly converted to aromatic carbon form. It could also be observed from TG graph (Supplementary information - Fig. S3) that during the pyrolysis, the organic compounds were lost massively before 500 °C, while the mass of the sample changed little from 500 °C to 800 °C. Overall, the NMR and IR results demonstrated that the organic functionality of CSCs keeps changing by the adjustment of carbonization temperature (described in Fig. 1). This is a unique advantage compared to the carbon-silica composite prepared through other methods which only prepared single functionality composites. It is worthwhile to note that no resonance signal ascribed to C-Si bond was detected as explained by ^{29}Si NMR spectra (see Supplementary information - Fig. S4).⁴³ Further work is needed to explore the possibility of silicon-carbide formation at higher temperatures above 1000 °C.

Table 1 Chemical Shifts ($\Delta\delta$) in the spectra of ^{19}F solid state NMR of SBA-15 materials carbonized at 500 °C, 600 °C and 800 °C, CSC materials carbonized at 300 °C, 400 °C, 500 °C, 600 °C and 800 °C and activated carbon materials.

Sample No.	$\Delta\delta$	Sample No.	$\Delta\delta$
CSC-300	3.14	Activated carbon	-4.61
CSC-400	3.1	SBA-15-500	2.64
CSC-500	2.88	SBA-15-600	2.75
CSC-600	2.62	SBA-15-800	2.92
CSC-800	2.16		

Previous work demonstrated the utility of fluorine-containing compounds as probe molecules to investigate the surface functionality.⁴⁴ Using ^{19}F NMR, the chemical shift difference ($\Delta\delta$) between the characteristic peak of fluorine in the liquid-phase peak and on the material surface correlates well with both surface energy and polarity values of the materials.⁴⁴ The pure carbon material contains an electron-rich graphite-like structure, which contributes greatly to surface energy value, thus resulting in a significant chemical shift, compared to pure silica material. Table 1 shows the chemical shifts in the spectra of ^{19}F solid state NMR of SBA-15 materials heated at 500 °C, 600 °C and 800 °C, CSC materials carbonized at 300 °C, 400 °C, 500 °C, 600 °C and 800 °C and commercial activated carbon (activated charcoal Norit[®], from coal) samples. The chemical shifts of CSC materials decrease and move towards the value for activated carbon (-4.61 ppm) with the increase of pyrolysis temperature, indicating that the surface functionality of composites tend to become more like that of

carbon species. This is due to the high temperature CSCs containing greater percentage of graphitic or polyaromatic carbon species (CSC-600 & CSC-800), which is in agreement with ^{13}C NMR results. The fluorine peak of CSC-300 on the material surface is sharp and intensive (Supplementary information - Fig. S5), indicating that the carbonaceous layer distribute uniformly on the silica pores. Due to the decomposition of organic compounds with the increase of temperature, the thickness of this carbonaceous layer decreases, resulting in the low intensity peaks for high temperature samples. Besides, the SBA-15 materials have an increased chemical shift with the increase of temperature, demonstrating high temperature leads to a more polar SBA-15 material because of the further crosslink effect between silica and silica species. It is noteworthy to highlight that the chemical shifts of CSCs prepared at 300 and 400 °C are even higher than that of parent SBA-15, suggesting that a more hydrophilic surface was prepared at lower pyrolysis temperature. This is due to most of polar organic carbon-containing compounds still remaining in the composites, leading to polar materials – indeed the ^{13}C NMR data suggests a product rich in hydroxyl groups and carbonyl species. Such a kind of functionalized silica materials with highly polarity could have a potential in some specific separation process except CSC-300 material with poor porosity and low surface area.

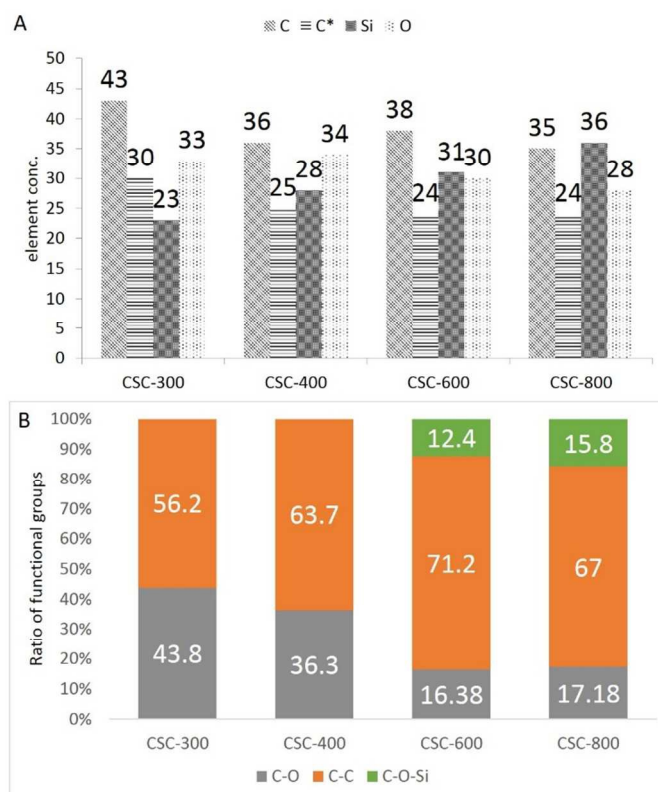


Fig. 5 A) Graph of C, Si and O element concentration for CSC materials from XPS analysis except C* column stands for the data from CHN analysis. B) Ratios of C-O, C-C and C-O-Si groups in CSC-300, CSC-400, CSC-600 and CSC-800

The C, Si and O elemental composition for CSCs was measured by XPS and CHN analysis (Fig. 5A). Increasing pyrolysis temperature generally results in a decrease in the %C and an increase in the %Si, providing further proof of loss of carbon-containing compounds at high pyrolysis temperature. The carbon concentration detected from CHN analysis for all CSCs was much lower than that from XPS analysis, which is consistent with the surface sensitivity of XPS.⁴¹ This further supports a model in which the surface of the composites is a carbon-rich layer due to carbon species coating the walls of the silica support as previously described in Fig. 1. A series of spectra for the C_{1s} core level peaks of the CSCs prepared at 300 °C, 400 °C, 600 °C and 800 °C is shown in Fig. 6. Three contributions can be identified due to: C-C group, C-O group (C-O-C or C-O-H) and C-O-Si group at 284.4 eV, 285.7 eV and 288.9 eV binding energies, respectively.^{41, 45} The dominant peak in these samples is attributed to C-C group. The intensity of the peak observed at 285.7 eV tends to decrease as the increase of temperature as a result of the loss of organic compounds. It is clear to observe that the C-C/C-O ratio keeps increasing with the increase of temperature (Fig. 5B). This result is consistent with DRIFT and carbon NMR data, showing a temperature-dependent functionalized CSC was synthesized.

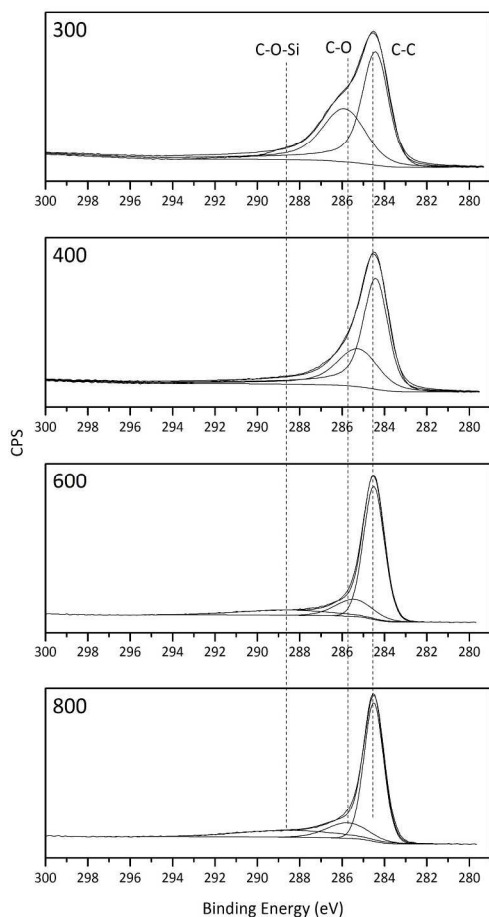


Fig. 6 C_{1s} XPS spectra of CSC-300, CSC-400, CSC-600 and CSC-800 samples

It is worthwhile to note that the appearance of a small and broad peak at 288.9 eV is assigned to C-O-Si species.⁴¹ This could be attributed to the interactions between bio-oils and silicas,⁴⁶ demonstrating the feasibility of carbon-silica composite fabrication by using bio-oil and silica. In addition, previous research reported that waste ash obtained from combustion of bio-char, which is generated from microwave of biomass, could be converted into structured mesoporous silicas.⁴⁷ Thus by combining these two approaches together, a comprehensive utilization of waste biomass from microwave pyrolysis to prepare mesoporous carbonaceous silica materials is proposed here (see Supplementary information - Fig. S6).

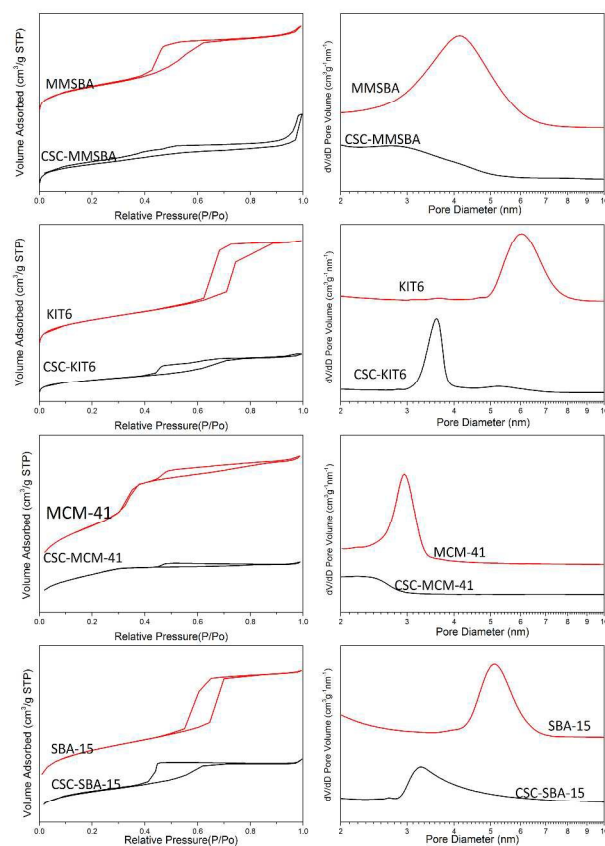


Fig. 7 N₂ adsorption/desorption isotherm plots and pore size distribution of parent MMSBA, KIT-6, MCM-41, SBA-15 and corresponding modified CSCs

Utilization of other types of silica substrates

Three different mesoporous silicas including MCM-41, macroporous-mesoporous SBA-15 (MMSBA) and KIT-6 were utilized in this synthesis approach and their respective composites were characterized in this work. MCM-41 is a popular and classic silica material, possessing a hexagonal arrangement of uniformly sized mesopores (1-10 nm).⁴⁸ MMSBA with meso-macro porous structure and KIT-6 with interconnected pore network exhibited improved pore interconnectivity and enhanced pore accessibility, allowing for

a better mass transport compared to conventional SBA-15. MMSBA, which was synthesized via dual-templating routes employing P123 and polystyrene beads, had advantages of high surface areas and interconnecting macro- and mesopore networks with respective narrow pore size distributions.^{35, 49} KIT-6 possesses highly accessible and highly connected open porous networks due to its unique cubic *1a3d* pore architecture.^{50, 51}

All of these porous silicas could be utilized in the preparation of carbon-silica composites with unique pore matrixes, offering vast prospects for future applications. The similar XRD patterns (Supplementary information - Fig. S7) of three silicas and respective composites revealed that the CSCs contained the same mesostructure as their parent silicas. Porosimetry results (Fig. 7) are in good correlation with XRD data and also proved that the CSCs were successfully prepared via this method. Similarly to SBA-15 result, the pore volumes and the average pore diameters of the corresponding CSCs decreased after bio-oil modification of these silica substrates (Supplementary information - Table S3). Due to the smaller average pore diameter of MMSBA (4.2 nm) and MCM-41 (3.2 nm) compared to SBA-15 (5.1 nm), the mesopores would coat with carbonaceous layer, resulting in a smaller pore size less than 2 nm (micropore size) after the modification. Comparison between the porosimetry data of original parent silicas and CSC materials can be viewed in supporting information Table S3.

Notably a ratio of material's surface area (SA) or pore volume and bio-oil amount plays an important role in tailoring the thickness of carbonaceous layer and pore size of CSC. Resulting from the high ratio of bio-oil to SA in MMSBA and MCM-41, a thicker carbon layer on the walls and smaller pore sizes were obtained, ultimately leading to a structure full of organics and more like CSC-300. Hence, the investigation between SA/bio-oil ratio and material's property should be further developed.

Conclusions

In conclusion, the CSCs have been synthesized successfully via modifying the surface of a range of mesostructured silicas with bio-oil (generated from the pyrolysis of waste paper) as carbon source. The synthesized composites possess a continuum of functionalities ranging from polar hydroxyl groups to aromatic surfaces through simply adjusting pyrolysis temperature. After the modification process, structural characterizations reveal that the resultant CSCs exhibit well-ordered structures with high specific BET surface area, uniform pore sizes, comparable with the parent silicas. The chemical property and surface functionality of CSCs could be controlled by carbonization temperature, offering this composite a variety of potential applications in chemical separation and heterogeneous catalysis. Owing to the well-ordered mesostructure, high surface area and variable surface functionality of CSCs, they may find use in a wide variety of potential applications including separation processes, chromatography and heterogeneous catalysis.

Acknowledgements

We would like to thank Dr. Meg Stark for the TEM imaging, Dr. Mark Isaacs at EBRI, Aston University for XPS measurements and Dr. David Apperley (EPSRC Solid State NMR service, Durham University) for assistance measuring the solid state NMR data.

Notes and references

^a Green Chemistry Centre of Excellence, Department of Chemistry, University of York, YO10 5DD, UK. E-mail: andrew.hunt@york.ac.uk

^b Departamento de Física de Polímeros, Elastómeros y Aplicaciones Energéticas, Instituto de Ciencia y Tecnología de Polímeros, CSIC, c/ Juan de la Cierva, 3, 28006, MADRID, Spain.

^c European Bioenergy Research Institute (EBRI), Aston University, Birmingham, B4 7ET, UK.

Electronic Supplementary Information (ESI) available: See DOI: 10.1039/b000000x/

1. J. Wang, C. Xiang, Q. Liu, Y. Pan and J. Guo, *Adv. Funct. Mater.*, 2008, **18**, 2995.
2. R. Ryoo, S. H. Joo, M. Kruk and a. M. Jaroniec, *Adv. Mater.*, 2001, **13**, 677.
3. S. Jun, S. H. Joo, R. Ryoo, M. Kruk, M. Jaroniec, Z. Liu, T. Ohsuna and O. Terasaki, *J. Am. Chem. Soc.*, 2000, **122**, 10712.
4. S. H. Joo, S. Jun and R. Ryoo, *Microporous Mesoporous Mater.*, 2001, **44-45**, 153.
5. A.-H. Lu, W. Schmidt, N. Matoussevitch, H. Bönemann, B. Spliethoff, B. Tesche, E. Bill, W. Kiefer and F. Schüth, *Angew. Chem. Int. Ed.*, 2004, **43**, 4303.
6. G. Liu, S. Zheng, D. Yin, Z. Xu, J. Fan and F. Jiang, *J. Colloid Interface Sci.*, 2006, **302**, 47.
7. M. Choi and R. Ryoo, *Nat Mater.*, 2003, **2**, 473.
8. S. H. Joo, S. J. Choi, I. Oh, J. Kwak, Z. Liu, O. Terasaki and R. Ryoo, *nature*, 2001, **412**, 169.
9. J. Lee, S. Han and T. Hyeon, *J. Mater. Chem.*, 2004, **14**, 478.
10. J. Lee, J. Kim and T. Hyeon, *Adv. Mater.*, 2006, **18**, 2073.
11. G. Du, Y. Zhou and B. Xu, *Mater. Charact.*, 2010, **61**, 427.
12. Y. Y. Tsai, J. S. Su, C. Y. Su and W. H. He, *J. Mater. Process. Technol.*, 2009, **209**, 4413.
13. J. Prasek, J. Drbohlavova, J. Chomoucka, J. Hubalek, O. Jasek, V. Adam and R. Kizek, *J. Mater. Chem.*, 2011, **21**, 15872.
14. M. Si, D. Feng, L. Qiu, D. Jia, A. A. Elzatahry, G. Zheng and D. Zhao, *J. Mater. Chem. A*, 2013, **1**, 13490.
15. L. Song, D. Feng, C. G. Campbell, D. Gu, A. M. Forster, K. G. Yager, N. Fredin, H.-J. Lee, R. L. Jones, D. Zhao and B. D. Vogt, *J. Mater. Chem.*, 2010, **20**, 1691.
16. R. Liu, Y. Shi, Y. Wan, Y. Meng, F. Zhang, D. Gu, Z. Chen, B. Tu and D. Zhao, *J. Am. Chem. Soc.*, 2006, **128**, 11652.
17. M. Sevilla, C. Falco, M.-M. Titirici and A. B. Fuertes, *RSC Adv.*, 2012, **2**, 12792.
18. M.-M. Titirici, R. J. White, C. Falco and M. Sevilla, *Energ. Environ. Sci.*, 2012, **5**, 6796.
19. E. Thompson, A. Danks, L. Bourgeois and Z. Schnepf, *Green Chem.*, 2015, **17**, 551.
20. M. E. Miller and R. Wool, in *APS Meeting Abstracts*, 2006, p. 25007.
21. T. G. Glover, K. I. Dunne, R. J. Davis and M. D. LeVan, *Microporous Mesoporous Mater.*, 2008, **111**, 1.
22. F. de Clippel, A. Harkiolakis, X. Ke, T. Vösch, G. Van Tendeloo, G. V. Baron, P. A. Jacobs, J. F. Denayer and B. F. Sels, *Chem. Commun. (Cambridge, U. K.)*, 2010, **46**, 928.
23. B. Charmas, R. Lebeda, S. Pikus, A. Jezierski and E. Kobylas, *Colloids and Surfaces A: Physicochem. Eng. Aspects*, 2002, **208**, 93.
24. J. Shen, M. Wang, Y. Wu and F. Li, *RSC Adv.*, 2014, **4**, 21089.

25. Y. Pan, M. Ju, C. Wang, L. Zhang and N. Xu, *Chem. Commun.*, 2010, **46**, 3732.
26. H. Wang and J. Yao, *Ind. Eng. Chem. Res.*, 2006, **45**, 6393.
27. P. Rutkowski, *Fuel Process. Technol.*, 2011, **92**, 517.
28. A. Demirbas, *Energy Sources, Part A*, 2007, **29**, 753.
29. R. Lu, G.-P. Sheng, Y.-Y. Hu, P. Zheng, H. Jiang, Y. Tang and H.-Q. Yu, *Biomass Bioenergy*, 2011, **35**, 671.
30. D. Mohan, C. U. P. Jr. and P. H. Steele, *Energy Fuels*, 2006, **20**, 848.
31. Q. Lu, W.-Z. Li and X.-F. Zhu, *Energy Convers. Manage.*, 2009, **50**, 1376.
32. D. Zhao, Q. Huo, J. Feng, B. F. Chmelka and G. D. Stucky, *J. Am. Chem. Soc.*, 1998, **120**, 6024.
33. T.-W. Kim, F. Kleitz, B. Paul and R. Ryoo, *J. Am. Chem. Soc.*, 2005, **127**, 7601.
34. S. Vaudreuil, M. Bousmina, S. Kaliaguine and L. Bonnevot, *Adv. Mater.*, 2001, **13**, 1310.
35. J. Dhainaut, J.-P. Dacquin, A. F. Lee and K. Wilson, *Green Chem.*, 2010, **12**, 296.
36. C. Xue, B. Tu and D. Zhao, *Adv. Funct. Mater.*, 2008, **18**, 3914.
37. Z. Luan, J. A. Fournier, J. B. Wooten and D. E. Miser, *Microporous Mesoporous Mater.*, 2005, **83**, 150.
38. P. Shah and V. Ramaswamy, *Microporous Mesoporous Mater.*, 2008, **114**, 270.
39. Y. Usami, T. Hongo and A. Yamazaki, *J. Porous Mater.*, 2011, **19**, 897.
40. Y. Li, Y. Chen, L. Li, J. Gu, W. Zhao, L. Li and J. Shi, *Appl. Catal., A*, 2009, **366**, 57.
41. A. S. M. Chong and X. S. Zhao, *J. Phys. Chem. B*, 2003, **107**, 12650.
42. K. S. Novoselov, A. K. Geim, S. V. Morozov, D. Jiang, Y. Zhang, S. V. Dubonos, I. V. Grigorieva and A. A. Firsov, *Science*, 2004, **306**, 666.
43. Z. M. Wang, K. Hoshino, K. Shishibori, H. Kanoh and K. Ooi, *Chem. Mater.*, 2003, **15**, 2926.
44. V. L. Budarin, J. H. Clark and S. J. Tavener, *Chem. Commun. (Cambridge, U. K.)*, 2004, 524.
45. A. Avila, I. Montero, L. Galán, J. M. Ripalda and R. Levy, *J. Appl. Phys.*, 2001, **89**, 212.
46. N. W. Smith and M. B. Evans, *Chromatographia*, 1995, **41**, 197.
47. J. R. Dodson, E. C. Cooper, A. J. Hunt, A. Matharu, J. Cole, A. Minihan, J. H. Clark and D. J. Macquarrie, *Green Chem.*, 2013, **15**, 1203.
48. C.-Y. Chen, H.-X. Li and M. E. Davis, *Microporous Mater.*, 1993, **2**, 17.
49. J.-P. Dacquin, J. Dhainaut, D. Duprez, S. Royer, A. F. Lee and K. Wilson, *J. Am. Chem. Soc.*, 2009, **131**, 12896.
50. F. Kleitz, S. Hei Choi and R. Ryoo, *Chem. Commun.*, 2003, 2136.
51. C. Pirez, J.-M. Caderon, J.-P. Dacquin, A. F. Lee and K. Wilson, *ACS Catalysis*, 2012, **2**, 1607.

The table of contents entry

Carbon-silica composites have been successfully synthesized through the carbonization of mesoporous silica with microwave pyrolysis bio-oils. The resultant CSC exhibits not only similar pore structural ordering, but also unique advantages including temperature-dependent surface functionality, cost-effective carbon source from waste.

*Tengyao Jiang, Vitaliy L. Budarin, Peter S. Shuttleworth, Gary Ellis, Christopher M.A. Parlett, Karen Wilson, Duncan J. Macquarrie and Andrew J. Hunt**

Keywords: carbon-silica composites, mesoporosities, bio-oils, continuum functionalities

Title: Green Preparation of Tunable Carbon-Silica Composite Materials from Wastes

